JACS
JOURNAL OF THE AMERICAN CHEMICAL SOCIETY
Communication
pubs.acs.org/JACS

Nitrogen-Doped Colloidal Graphene Quantum Dots and Their Size-Dependent Electrocatalytic Activity for the Oxygen Reduction Reaction

Qiqi Li,[†] Sheng Zhang,[‡] Liming Dai,[‡] and Liang-shi Li*,[†]

[†]Department of Chemistry, Indiana University, Bloomington Indiana 47405, United States

[‡]Department of Macromolecular Science and Engineering, Case Western Reserve University, Cleveland, Ohio 44106, United States

Supporting Information

ABSTRACT: Nitrogen doping has been a powerful way to modify the properties of carbon materials ranging from activated carbon to graphene. Here we report on a solution chemistry approach to nitrogen-doped colloidal graphene quantum dots with well-defined structures. N-doping was demonstrated to significantly affect the properties of the quantum dots, including the emergence of size-dependent electrocatalytic activity for the oxygen reduction reaction.

Nitrogen substitution, or substitutional N-doping, has been a powerful method to modify graphitic carbon materials for various applications, ranging from catalysis to microelectronics.[1,2] N-doped activated carbon or carbon nanotubes,[1,2] for example, possess catalytic activities for some important chemical reactions such as oxygen reduction and dehydrochlorination. In graphene, substitutional nitrogen atoms can significantly modify the electronic structures of the host,[3] providing a promising way to tailor the transport properties of graphene for electronic applications. However, N-doping of the carbon materials so far inevitably requires harsh reaction conditions such as high temperature or fields.[1] As a result, it is very difficult to control the distribution and bonding configurations of the nitrogen dopants in the π-conjugated framework, leading to a poor understanding about the doping effects and ill-controlled material properties. Herein, we report on a solution chemistry approach to N-doped colloidal graphene quantum dots (QDs, **1** and **2** in Scheme 1). This approach has enabled us to synthesize the QDs with well-defined structures and various sizes. We further show that the incorporation of the nitrogen atoms significantly varies the properties of the resultant QDs. In particular, it was found that the N-doped QDs could electrochemically catalyze the oxygen reduction reaction with a size-dependent activity.

Scheme 1. Structures of N-Doped Graphene QDs 1, 2 and an Undoped QD 3 for Comparison Studies

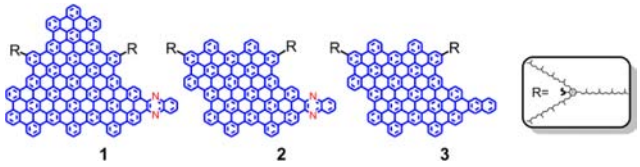

Colloidal graphene QDs are a new addition to zero-dimensional quantum-confined systems, and have some unique properties due to the dimensionality of graphene and the light constituent elements.[4] The graphene QDs are soluble in common organic solvents because of the peripheral trialkyl phenyl groups (R- groups in Scheme 1), which make a flexible, three-dimensional cage around the graphene core to prevent aggregation. Combining the solubilization method with well-developed reactions for carbon−carbon bond formation, we have synthesized various colloidal graphene QDs with uniform sizes and well-defined structures.[4]

In this work, we apply the solution chemistry approach to synthesis of graphene QDs doped with nitrogen atoms. In addition to two nitrogen atoms, the conjugated cores (marked blue in Scheme 1) of QDs **1** and **2** contain 176 and 128 carbon atoms, respectively. With the solution chemistry approach, we can not only control the numbers of nitrogen atoms in the QDs, but also define their bonding configurations so that **1** and **2** were made as aryl-annulated phenazines. This is in sharp contrast to those methods previously explored for doping graphene[1] and can afford graphene QDs with well-defined properties. To understand the doping effects in the QDs, we also synthesized QD **3**, an undoped analogue of **2**, which contains 130 conjugated carbon atoms in the graphene core (marked blue in Scheme 1). Because of the presence of the solubilizing R- groups, all the QDs are soluble in common solvents, such as toluene, tetrahydrofuran (THF), and chloroform.

The synthesis of **1**−**3** is outlined in Scheme 2. Briefly, we start with small substituted benzene derivatives such as 2-bromo-5-iodo-3′-(phenylethynyl)-1,1′-biphenyl (**4**) and phenylboronic acid to yield a nitrogen-containing intermediate **6** (details in the Supporting Information (SI)). Then **6** undergoes double Suzuki cross-coupling reactions, leading to **8** and **9**, the precursors for **1** and **2**, respectively. Upon treatment with a large excess of iron(III) chloride under a constant stream of argon in a dichloromethane/nitromethane mixture at room temperature,[4b] these precursors are converted to the N-doped graphene QDs. Similarly, QD **3** is obtained from an α, β-diketone **5** with the Wittig reaction,[5] followed by the Suzuki coupling and oxidative dehydrogenation. As for previously reported graphene QDs, the precursors **8**−**10** for **1**−**3** are

Received: September 18, 2012
Published: November 5, 2012

   dx.doi.org/10.1021/ja309270h | J. Am. Chem. Soc. 2012, 134, 18932−18935

Scheme 2. Synthesis of Quantum Dots 1−3[a]

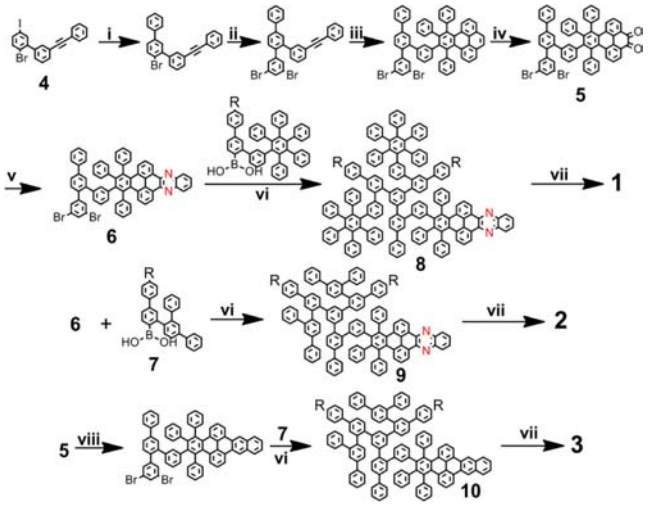

[a]Conditions: (i) phenylboronic acid, $Pd(PPh_3)_4$, K_2CO_3, toluene/EtOH/H_2O, 80 °C; (ii) (a) *n*-BuLi, THF, −78 °C, (b) 2-isopropoxy-4,4,5,5-tetramethyl-1,3,2-dioxaborolane, −78 °C to rt, (c) 1,3-dibromo-5-iodobenzene, $Pd(PPh_3)_4$, K_2CO_3, toluene/EtOH/H_2O, 85 °C; (iii) 9,11-diphenyl-10*H*-cyclop-enta[*e*]pyren-10-one, Ph_2O, 240 °C; (iv) $RuCl_3$, $NaIO_4$, CH_2Cl_2/CH_3CN/H_2O, rt; (v) benzene-1,2-diamine, EtOH/$CHCl_3$, 65 °C; (vi) $Pd(PPh_3)_4$, K_2CO_3, toluene/EtOH/H_2O, 80 °C; (vii) $FeCl_3$, CH_2Cl_2/CH_3NO_2, rt; (viii) *o*-Xylylenebis(triphenylphosphonium bromide), LiOH(aq, 5 M), CH_2Cl_2, rt.

purified with gel chromatography and characterized with standard organic characterization techniques. The final products **1**−**3** are purified with repetitive dissolution in toluene and precipitation with methanol. Their structures are confirmed with isotope-resolved MALDI-mass spectroscopy, showing excellent uniformity in size (Figure 1, details in the SI). It should be noted that the concentration control of oxidant iron(III) chloride is crucial for the success in the oxidative dehydrogenation step to yield **1** and **2**. The precursors cannot be fully oxidized unless the concentration of the oxidant is as high as 35 mg/mL in the dichloromethane/nitromethane mixture. A possible explanation is that, in the presence of the electron-withdrawing nitrogen atoms, a high concentration of the oxidant is necessary for the formation of cationic intermediates so that the dehydrogenation can go to completion.[6] The excess of the iron(III) chloride was completely removed by repetitive washing, as confirmed with X-ray photoelectron spectroscopy (shown in the SI).

The presence of the nitrogen atoms in QDs **1** and **2** dramatically affects their optical properties. Figure 2 shows

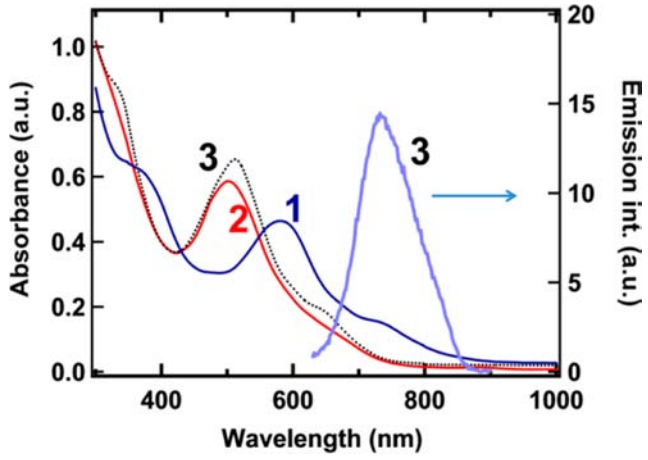

Figure 2. UV−vis absorption spectra of QDs **1**−**3** (left axis) and fluorescence spectrum of **3** (right axis) in THF.

UV−vis absorption spectra of **1**−**3** and the fluorescence spectrum of **3** (excited at 600 nm). As expected from their sizes, the absorption edge of **1** appears at a significantly longer wavelength than those of **2** and **3**, whereas **2** and **3** have almost the same absorption spectra with little differences. More strikingly, **3** is highly fluorescent, whereas **1** or **2** does not have detectable photoluminescence (Figure 2). This is consistent with the absence of n → π^*, the lowest-energy transitions, in the absorption spectra of **1** and **2**. The n → π^* transitions are expected for the N-substituted aromatic heterocycles and are indeed observed in their precursors (**8** and **9**) (see the SI). The large size of **1** and **2** explains the diminishing oscillator strengths of the n → π^* transitions, because of the decreasing orbital overlap between the increasingly delocalized π^* electrons and the nonbonding electrons localized on the nitrogen atoms. In contrast, the lowest-energy transition in **3** is π → π^*, which is responsible for the emission and has a less size-dependent oscillator strength.

The electrocatalytic activity of the N-doped graphene QDs for the oxygen reduction reaction (ORR) is of particular interest and thus has been investigated in our studies. There

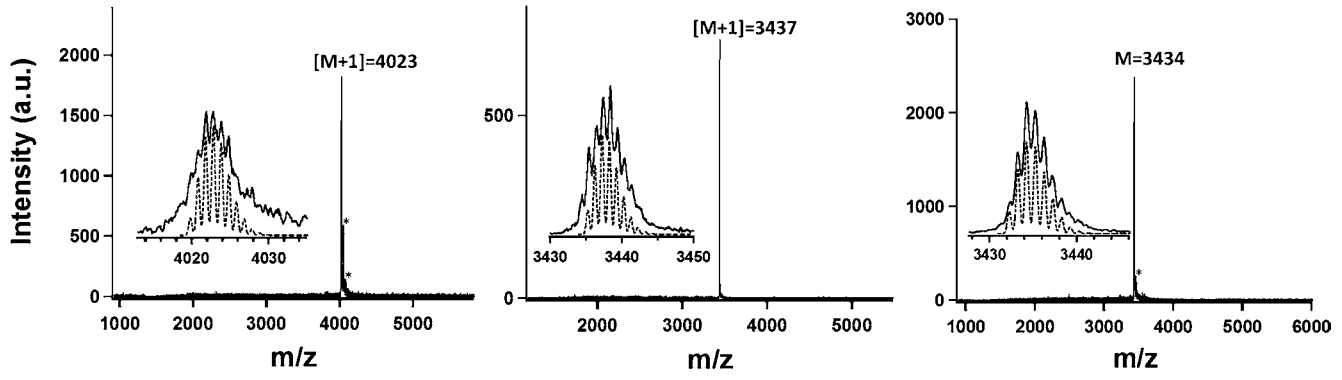

Figure 1. MALDI-TOF MS spectra of QDs **1**−**3** ([**1**+H]$^+$, [**2**+H]$^+$, and **3**$^+$, left to right), respectively. In the insets are the isotope-resolved patterns experimentally measured (solid curves) with ones calculated (dotted curves) from the molecular structures of the QDs. In the spectra for **1** and **3**, the small peaks marked by asterisks are due to chlorinated byproducts in the last oxidation step.[4b]

dx.doi.org/10.1021/ja309270h | *J. Am. Chem. Soc.* 2012, 134, 18932−18935

have been tremendous efforts on finding replacements for Pt to catalyze the ORR in fuel cells, and N-doped graphitic carbon materials are among the candidates being investigated.[2a,7] Figure 3a shows the cyclic voltammetry (CV) curves of **1** deposited on a glassy-carbon rotating disk electrode (RDE) in an O_2- or a N_2-saturated 0.1 M KOH aqueous solution (experimental details in the SI). A well-defined reduction peak occurs at around −0.3 V (vs SCE) in the O_2-saturated solution, whereas there is no such a peak in the N_2-saturated one, indicating that O_2 is reduced on the electrode coated with **1**.

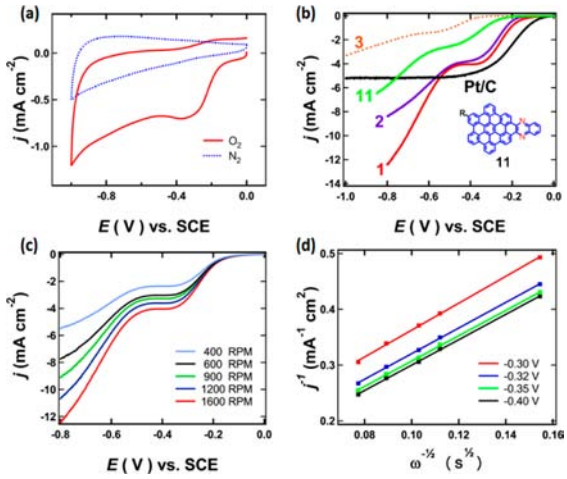

Figure 3. (a) CV curves (scanning rate of 50 mV s^{-1}) of **1** on a glassy-carbon RDE in a N_2- and an O_2-saturated 0.1 M KOH solution. (b) LSV curves (10 mV s^{-1}) for **1**−**3** and Pt/C on a RDE (1600 rpm) in an O_2-saturated 0.1 M KOH solution. Also shown is the LSV curve for **11**, a much smaller N-substituted heterocycle with structure shown in the inset. (c) LSVs (10 mV s^{-1}) for **1** on a RDE in an O_2-saturated 0.1 M KOH solution with various rotating speeds. (d) Koutecky−Levich plots for **1** obtained from the LSV curves in (c) at various voltage values. A global fitting of the plots reveals that the number of electrons transferred per O_2 molecule is 3.9.

Linear sweep voltammetry (LSV) shows that the N-doped QDs have high, size-dependent electrocatalytic activity for the ORR. Figure 3b shows the LSV curves obtained for QDs **1**−**3** and commercial Pt/C (20% wt. Pt on Vulcan XC-72R) of the same mass deposited on a glassy-carbon RDE in an O_2-saturated 0.1 M KOH aqueous solution (1600 rpm, experimental details in the SI). For further comparison, we also made a much smaller N-substituted aromatic compound **11** (Figure 3b), a derivative of hexabenzocoronene, and measured its LSV curve under the same condition. The N-containing **1**, **2**, and **11** show ORR onset potentials at −0.04, −0.10, and −0.14 V, respectively, relative to that for the commercial Pt/C catalyst. In addition, the cathodic current density increases with size of the QDs, indicating the improved catalytic activity of larger QDs. The more negative ORR onset potentials (and thus greater overpotentials) observed with the N-doped QDs than that with Pt/C, as well as the lower cathodic current densities with the same mass of the catalysts, indicate that the electrocatalytic activities of these N-doped QDs are not as good as that of Pt/C. Nevertheless, it is remarkable that the N-doped QDs lead to currents comparable with that by Pt/C, especially if we consider that the QDs have much greater molecular weights and thus we may expect fewer active sites[2] in the catalysts with the same mass. In contrast, the undoped QD **3** shows appreciable activity only at a much more negative potential (Figure 3b), illustrating the importance of the nitrogen doping, even at a level as low as ∼1% (N/C atomic ratio) in the conjugated framework, on the ORR activity. However, our results do not support the positive correlation between the catalytic activity and the nitrogen content that has been suggested previously.[2a,7] Rather, the largest N-doped QD **1** studied here, with the lowest doping level, shows the highest activity.

Further studies show that the ORR catalyzed by the N-doped graphene QDs can occur via a four-electron reduction pathway to produce water directly rather than the two-electron pathway with peroxide as the intermediate.[8] The LSV curves measured with a RDE with **1** at various rotating speeds are presented in Figure 3c, showing increasing catholic current at increasing rotating speeds due to improved mass transport at the electrode surface. From the slope of the Koutecky−Levich plots (Figure 3d) obtained from the data in Figure 3c, the number of electrons transferred per oxygen molecule in the ORR is calculated to be about 3.9 (see the SI), consistent with a four-electron process that have been reported for other N-doped carbon materials.[2a,7] Therefore, similar catalytic mechanisms may also apply to the graphene QDs investigated in the present study.

The size-dependent catalytic activity of the N-doped graphene QDs has important implications in understanding and further improving the catalytic activities of N-doped carbon materials. Previous work was based on a hypothetical correlation between the catalytic activity and the bonding configurations of nitrogen atoms in the carbon framework.[2a,7] Consequently, efforts mostly have been focused on increasing the abundance of nitrogen atoms with a specific bonding configuration, resulting in a debate on what configuration is optimal.[2a,7] Our studies clearly indicate the conjugation size in these materials as an important parameter that has largely been ignored. This size dependence is consistent with recent theoretical calculations,[9] and may be due to the higher HOMO levels in larger QDs which as a result can be more easily oxidized. Furthermore, since the solution chemistry approach presented herein should be applicable to the synthesis of QDs doped with nitrogen atoms in other bonding configurations,[1,2a] the N-doped colloidal graphene QDs could provide unique opportunities for systematically investigating the mechanisms of the catalyzed ORR by N-doped carbon materials.

■ ASSOCIATED CONTENT

Ⓢ Supporting Information

Detailed procedure for synthesis, characterization of intermediates for QDs **1**−**3** and **11**, electrochemical measurements and data analysis, absorption spectra of **8**−**10**. This material is available free of charge via the Internet at http://pubs.acs.org.

■ AUTHOR INFORMATION

Corresponding Author

li23@indiana.edu

Notes

The authors declare no competing financial interest.

■ ACKNOWLEDGMENTS

This work was supported by NSF (DMR-1105185). S. Zhang and L. Dai acknowledge the funds from NSF (CMMI-1000768) and AFOSR (FA9550-12-1-0037; FA2386-10-1-

4071). The mass spectroscopy measurements were conducted in the Mass Spectrometry Facility in the Department of Chemistry at Indiana University, Bloomington.

REFERENCES

(1) Boehm, H.-P. In *Carbon Materials for Catalysis*; Serp, P., Figueiredo, J. L., Eds.; John Wiley & Sons: Hoboken, NJ, 2009; pp 131−155; Liu, H.; Liu, Y.; Zhu, D. *J. Mater. Chem.* **2011**, *21*, 3335−3345. Wang, H.; Maiyalagan, T.; Wang, X. *ACS Catalysis* **2012**, *2*, 781−795.

(2) (a) Yu, D.; Nagelli, E.; Du, F.; Dai, L. *J. Phys. Chem. Lett.* **2010**, *1*, 2165−2173. (b) Gong, K.; Du, F.; Xia, Z.; Durstock, M.; Dai, L. *Science* **2009**, *323*, 760−764.

(3) Zhao, L.; He, R.; Rim, K. T.; Schiros, T.; Kim, K. S.; Zhou, H.; Gutiérrez, C.; Chockalingam, S. P.; Arguello, C. J.; Pálová, L.; Nordlund, D.; Hybertsen, M. S.; Reichman, D. R.; Heinz, T. F.; Kim, P.; Pinczuk, A.; Flynn, G. W.; Pasupathy, A. N. *Science* **2011**, *333*, 999−1003. Wang, X.; Li, X.; Zhang, L.; Yoon, Y.; Weber, P. K.; Wang, H.; Guo, J.; Dai, H. *Science* **2009**, *324*, 768−771.

(4) (a) Li, L.-S.; Yan, X. *J. Phys. Chem. Lett.* **2010**, *1*, 2572−2576. Yan, X.; Li, L.-S. *J. Mater. Chem.* **2011**, *21*, 3295−3300. (b) Yan, X.; Cui, X.; Li, B.; Li, L.-S. *Nano Lett.* **2010**, *10*, 1869−1873. Yan, X.; Cui, X.; Li, L.-S. *J. Am. Chem. Soc.* **2010**, *132*, 5944−5945. Yan, X.; Li, B.; Cui, X.; Wei, Q.; Tajima, K.; Li, L.-S. *J. Phys. Chem. Lett.* **2011**, *2*, 1119−1124.

(5) Yang, C.; Yang, D. T. C.; Harvey, R. G. *Synlett* **1992**, 799−800.

(6) Lambert, C.; Noll, G. *Angew. Chem., Int. Ed. Engl.* **1998**, *37*, 2107−2110. Lambert, C.; Noll, G. *J. Am. Chem. Soc.* **1999**, *121*, 8434−8442. Rempala, P.; Kroulik, J.; King, B. T. *J. Org. Chem.* **2006**, *71*, 5067−5081.

(7) Matter, P. H.; Zhang, L.; Ozkan, U. S. *J. Catal.* **2006**, *239*, 83−96. Chen, Z.; Higgins, D.; Tao, H.; Hsu, R.; Chen, Z. *J. Phys. Chem. C* **2009**, *113*, 21008−21013. Qu, L.; Liu, Y.; Baek, J.-B.; Dai, L. *ACS Nano* **2010**, *4*, 1321−1326. Kundu, S.; Nagaiah, T. C.; Xia, W.; Wang, Y.; Van Dommele, S.; Bitter, J. H.; Santa, M.; Grundmeier, G.; Bron, M.; Schuhmann, W. M.; Muhler, M. *J. Phys. Chem. C* **2009**, *113*, 14302−14310. Rao, C. V.; Cabrera, C. R.; Ishikawa, Y. *J. Phys. Chem. C* **2010**, *1*, 2622−2627. Liu, R.; Wu, D.; Feng, X.; Mullen, K. *Angew. Chem., Int. Ed.* **2010**, *49*, 2565−2569. Li, Y.; Zhao, Y.; Cheng, H.; Hu, Y.; Shi, G.; Dai, L.; Qu, L. *J. Am. Chem. Soc.* **2012**, *134*, 15−18. Luo, Z.; Lim, S.; Tian, Z.; Shang, J.; Lai, L.; MacDonald, B.; Fu, C.; Shen, Z.; Yu, T.; Lin, J. *J. Mater. Chem.* **2011**, *21*, 8038. Fellinger, T.-P.; Hasché, F.; Strasser, P.; Antonietti, M. . *J. Am. Chem. Soc.* **2010**, *134*, 4072.

(8) Yeager, E. *Electrochim. Acta* **1984**, *29*, 1527−1537.

(9) Zhang, L.; Xia, Z. *J. Phys. Chem. C* **2011**, *115*, 11170−11176. Wang, S.; Zhang, L.; Xia, Z.; Roy, A.; Chang, D. W.; Baek, J. B.; Dai, L. *Angew. Chem., Int. Ed.* **2012**, *51*, 4209−4212.